Vol. 7, No. 3, 2013 Chemistry

Oleg Figovsky[1], Dmitry Pashin[2], Zufar Khalitov[2], Diana Valeeva[2] and Andrey Chkanov[2]

THE CYLINDRICAL SUPERLATTICES SnS/SnS_2: MODEL OF STRUCTURE AND DIFFRACTION

[1] International Nanotechnology Research Center "Polymate", Migdal Haemek 23100, Israel
[2] Kazan National Research Technical University, 10, K. Marx str., Kazan, Tatarstan 420111, Russia
pashin@addnano.ru

Received: September 03, 2012 / Revised: November 02, 2012 / Accepted: February 15, 2013

© Figovsky O., Pashin D., Khalitov Z., Valeeva D., Chkanov A., 2013

Abstract. The cylindrical superlattices are realized on a basis of mixed-layer nanotubes SnS/SnS_2. The superperiod is formed due to the longitudinal goffering of nanotubes structure as a result of lattices disproportion of cylindrical layers SnS and SnS_2. The simple model of structure is proposed, specific diffraction effects are analyzed.

Keywords: nanotube, goffered nanotube, superlattice.

1. Introduction

The misfit mixed-layer nanotubes SnS_2/SnS with different degrees of order in cylindrical layers SnS_2 and SnS alternation were synthesized in the Weizmann Institute of Science (Israel) by R. Tenne group [1]. Nanotubes were synthesized on the basis of flat layered crystals SnS_2 by extraction of a part of S atoms forming SnS layers. The misfit of SnS_2 and SnS layers having not only different parameters of lattices but also layer symmetry results in a curvature of flat packs and forming nanotubes.

During an experimental research the nanotubes with rather original structure were found. The periodical alternation in a longitudinal direction of nanotube light and dark radial (or nearly radial) strips was observed at the TEM-images (Figs. 1 and 2). More detailed analysis of the TEM-images has shown that within the strips the layers have a wavy character, and the radius of layers curvature is approximately constant. Hence, to coordinate the lattices the nanotubes layers are bent not only in the cylinder circle direction, but also in the direction of its axis, forming goffered nanotube in such a way. Originally such nanotubes were named "strained", however the term "goffered" is more right for the structure character.

It is obvious, that such way of coordination is possible only for the layers with close longitudinal (along a nanotube axis) parameters of lattices a [2]. The analysis of microdiffraction patterns has shown that two types of SnS_2 layers always take place in SnS_2/SnS nanotubes: with a = 0.36 nm and developed on $\pi/2$ with a = 0.63 nm, while the parameter a of SnS layer is equal to 0.58 nm. Apparently, the additional bend in the nanotube axis direction arises in a pair of SnS_2 and SnS layers, where the SnS_2 layer has a = 0.63 nm. This layer is positioned on the external side of the bend. Really, the goffering takes place only in mixed-layer nanotubes OT (O – SnS layer, T – SnS_2 layer) and is absent in OTT or OTOTT structures, where the presence of an additional SnS_2 layer interferes with a bend.

The "additional" layer lines with reflexes are distinctly observed in the microdiffraction patterns of goffered nanotubes (Figs. 1 and 2). Similar additional layer lines located close to the basic ones are known in superlattices diffraction researches. It allows to offer the model of nanotube structure, based on a wavy superlattice in a longitudinal direction, and to apply the known approaches to interpretate its diffraction pattern. The measurements have shown that the inverse value of distance Δ_s from the basic layer line up to the additional one (Fig. 1) well corresponds to longitudinal periodicity in the TEM-image equal to 5.4 nm, the same as in the usual superlattices.

The microdiffraction patterns in Figs. 1 and 2 are rather similar; however there is an essential difference. The distribution of additional layer line intensity near the basic layer line 20l in Fig. 1 is similar to a profile of the basic line. The analogous distributions of the goffered nanotube on the microdiffraction pattern in Fig. 2 have obvious displacements in the nanotube axis direction.

Interpretation of this effect requires theoretical research of the problem. At first let us consider positions of the lattice sites of circular orthogonal [2] goffered nanotube, shown in Fig. 3 with the basic designations, and basic features of diffraction in it.

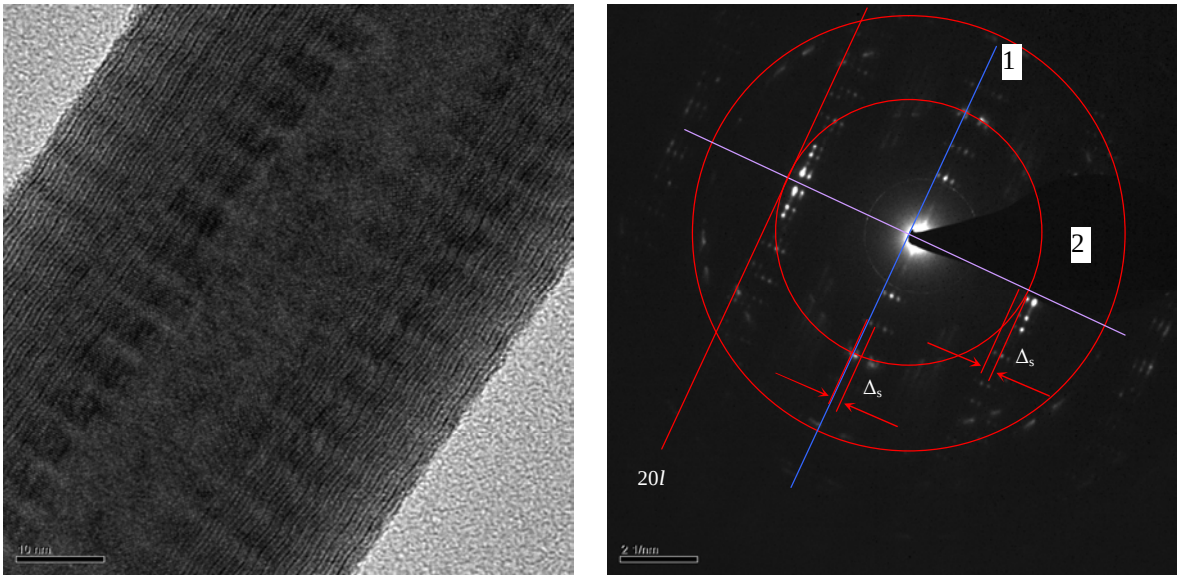

Fig. 1. TEM-image, microdiffraction pattern and sublattices scheme of SnS_2-SnS nanotube with thick radial CSR: zero layer line (1) and nanotube axis (2)

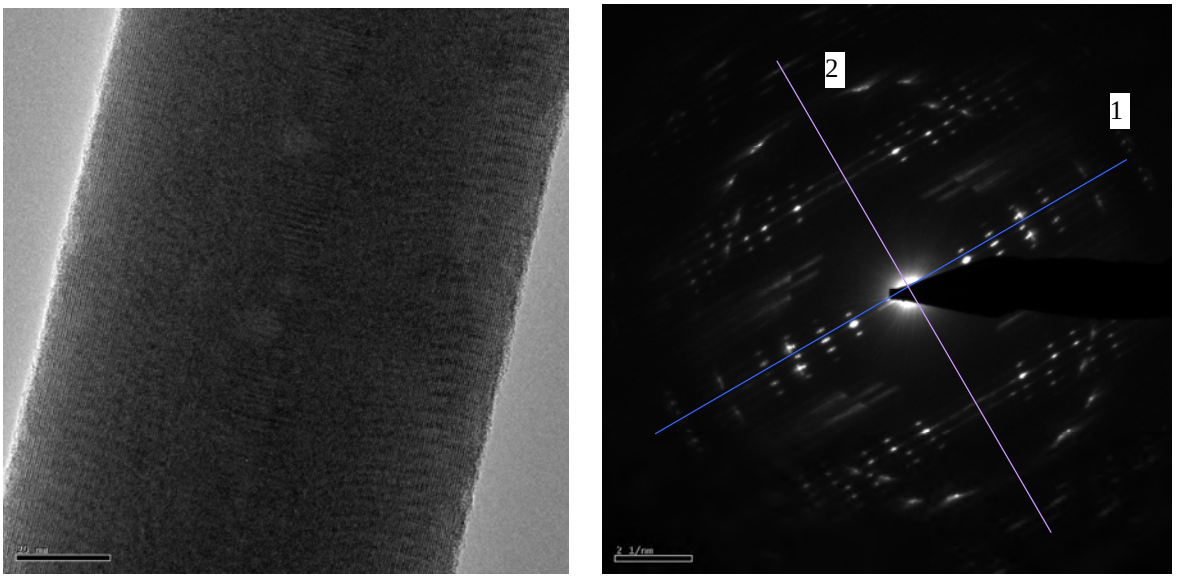

Fig. 2. TEM-image and microdiffraction pattern of SnS_2-SnS nanotube with thin radial CSR: zero layer line (1) and nanotube axis (2)

2. The Lattice of Goffered Nanotube

Let nanotube, oriented along z axis, consist of the ordered alternating "goffered" pairs of layers of A and B type, having the superperiod λ and the radius of the goffer bend r_g. Let both layers of every m-th pair have the same centre of goffer curvature located on the radius circle O_m (Fig. 3). Let the radius of internal layer point mostly remote from nanotube axis be equal to ρ_0, d_A and d_B – thickness of layers A and B, correspondingly, and $d = d_A + d_B$.

The discussed way of the coordination means that $\Delta\varepsilon$, an angle, under which the coordinated cell of layers pair is visible from the centre of pair curvature, becomes the crystallographic constant. Longitudinal parameter a of a lattice of coordinated layers pair has no definite value and for convenience can be chosen on an internal surface of the pair.

Let us number the sites of lattice formed by pairs within the limits of superlattice wave by integer variable t, and waves – by n. Then the angular position ε_t of any pair

sites concerning their curvature centre is possible to write as:

$$e_t = \Delta e\, t - e \qquad t = 0 \div T-1$$

where $\Delta e = \dfrac{a}{r_g}$ $e = \arcsin\dfrac{l}{2\left(r_g + d\right)}$

and coordinates of these sites and number of cells on the length of wave as:

$$z_{nt} = n l + \frac{l}{2} + r_g \sin e_t \quad T = \frac{2 r_g e}{a} \tag{1}$$

under obvious condition $l \le 2r_g$.

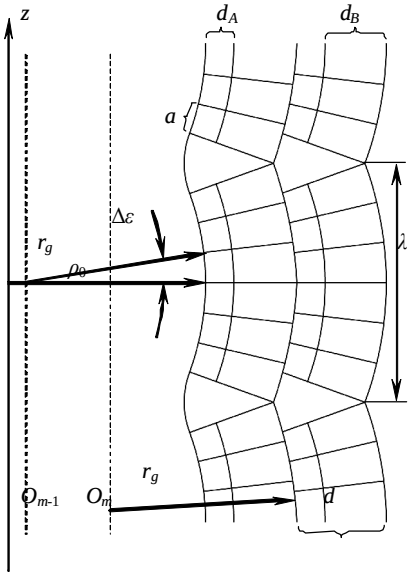

Fig. 3. The basic designations in the goffered nanotube

Radius of circles, on which the curvature centres of an internal layer waves are located, is equal to $\rho_0 - r_g$. Hence, it is possible to write down the polar radiuses of considered lattice sites as:

$$r_{mt} = r_m - r_g + r_g \cos e_t, \quad r_m = r_0 + md \tag{3}$$

Hence we can find an angle, under which the circular parameter b at $\varepsilon_t = 0$ is seen from the nanotube axis, and then – the angular positions of sites:

$$j_{mv} = \frac{b}{r_m} v + e_m \qquad v = 0 \div p_m - 1 \tag{4}$$

$$p_m = \frac{2\pi r_m}{b}$$

where v – the number of site on the circle; p_m – the number of sites on the m-th pair circles (integer by definition), ε_m – the initial azimuthal angular phase of the appropriate layer. It is obvious, that the circular parameter b has some variations within the limits of superlattice wavelength λ in the considered model. However it is known [3] that this parameter does not influence the circular nanotube strong reflexes ($k = 0$), consideration of which is the purpose of research.

3. The Strong Reflexes Amplitude

Let us write down an amplitude of diffraction by lattice, defined by the expressions (1), (3) and (4), in cylindrical coordinates system $\{R, \varphi^*, z^*\}$ in reciprocal space:

$$A(R, j^*, z^*) = \sum_{m,n,v,t} \exp\left\{2\pi i\left[R r_{mt} \cos\left(j_{mv} - j^*\right) + z_{nt} z^*\right]\right\} =$$

$$= \sum_{n=0}^{N-1} \exp\left(2\pi i\, l\, z^* n\right) \sum_{t=0}^{T-1} \exp\left[2\pi i\left(\frac{l}{2} + \right.\right.$$

$$\left.\left. + b_t\right) z^*\right] \sum_{m=0}^{M-1} \sum_{v=0}^{p_m - 1} \exp\left[2\pi i R r_{mt} \cos\left(j_{mv} - j^*\right)\right] \tag{5}$$

where $b_t = r_g \sin e_t$ (6)

M and N – the number of layer pairs in the nanotube and its length (in units λ), correspondingly. The sum over goffer periods (over n) is easily calculated and has the sharp maxima, equal to N, at

$$p\, l\, z^* = h_1 p \qquad \Rightarrow \qquad z^* = \frac{h_1}{l} \qquad h_1 = 0, \pm 1, \pm 2, \ldots . \tag{7}$$

The expression (7) defines the system of layer planes in the reciprocal space, on which all sites of reciprocal lattice take place. In the plane $\{R, z^*\}$, that is in the section of these planes by Evald sphere corresponding to the usual electron microdiffraction experiment, it gives the system of close located to each other layer lines (7), which numbering is the same with values of index h_1. Let limit by half plane $z^* \ge 0$, that means $h_1 \ge 0$.

With taking into account (7) the amplitude transforms in:

$$A(R, j^*, h_1) = N(-1)^{h_1} \sum_{t=0}^{T-1} \exp\left(2\pi i \frac{h_1}{l} b_t\right) \cdot$$

$$\cdot \left| \sum_{m=0}^{M-1} \sum_{v=0}^{p_m - 1} \exp\left[2\pi i R r_{mt} \cos\left(j_{mv} - j^*\right)\right] \right| \tag{8}$$

Let us expand the second exponent of (8) into a series of cylindrical waves according to:

$$\exp(ia\cos\gamma) = J_0(a) + 2\sum_{q=1}^{\infty} i^q \cos(q\gamma) J_q(a) \tag{9}$$

$$A(R, j^*, h_1) = N(-1)^{h_1} \cdot$$

$$\cdot \sum_{t=0}^{T-1} \exp\left(2\pi i \frac{h_1}{l} b_t\right) \sum_{m=0}^{M-1} J_0\left(2\pi R r_{mt}\right) \sum_{v=0}^{p_m - 1} 1 +$$

$$+ 2N(-1)^{h_1} \sum_{t=0}^{T-1} \exp\left(2\pi i \frac{h_1}{l} b_t\right) \sum_{m=0}^{M-1} \sum_{v=0}^{p_m - 1} \sum_{q=1}^{\infty} i^q \cdot$$

$$\cdot \cos\left[q\left(j_{mv} - j^*\right)\right] J_q\left(2\pi R r_{mt}\right) = A_S + A_D$$

where, in view of triviality of the sum over *v*, the first addendum looks like:

$$A_S(R,h_1) = N(-1)^{h_1}$$

$$\sum_{t=0}^{T-1}\exp\left(2p\,i\frac{h_1}{l}b_t\right)\sum_{m=0}^{M-1}p_m J_0(2p\,R\,r_{mt}) \qquad (10)$$

and gives the amplitude of the so-called "strong " reflexes [3].

With the purpose of estimation of strong reflexes intensity distribution let's approximate the Bessel function in (10) by cosine $J_0(x) \approx \sqrt{\frac{2}{p\,x}}\cos x$ and neglecting the dependence of *t* on a radical, change the sums by places:

$$A_S(R,h_1) \approx N(-1)^{h_1}\sum_{m=0}^{M-1}\frac{p_m}{p\sqrt{R\,r_m}}\sum_{t=0}^{T-1}\exp\left(2p\,i\frac{h_1}{l}b_t\right)\cos(2p\,R\,r_{mt})$$

Let us consider the sum over *t*, presenting cosine in an exponential form:

$$\frac{1}{2}\sum_{t=0}^{T-1}\exp\left(2p\,i\frac{h_1}{l}b_t\right)\left[\exp(2p\,iR\,r_{mt})+\right.$$

$$\left.+\exp(-2p\,iR\,r_{mt})\right] = \frac{1}{2}(S_1+S_2),$$

where $S_1 = \sum_{t=0}^{T-1}\exp\left[2p\,i\left(\frac{h_1}{l}b_t + R\,r_{mt}\right)\right]$

$$S_2 = \sum_{t=0}^{T-1}\exp\left[2p\,i\left(\frac{h_1}{l}b_t - R\,r_{mt}\right)\right] \qquad (11)$$

With regard to (3) and (6), the sum S_1:

$$S_1 = \exp\left[2p\,iR\left(r_0 - r_g + md\right)\right]\cdot$$

$$\cdot\sum_{t=0}^{T-1}\exp\left[2p\,ir_g\frac{h_1}{l}\sin(\Delta e\,t - e)\right]\cdot$$

$$\cdot\exp\left[2p\,ir_g R\cos(\Delta e\,t - e)\right] \qquad (12)$$

Let us expand two last exponents into a series of cylindrical waves according to:

$$\exp(ia\sin g) = J_0(a) + 2\sum_{q=1}^{\infty}\cos(2qg)J_{2q}(a) +$$

$$+ 2i\sum_{q=0}^{\infty}\sin[(2q+1)g]\,J_{2q+1}(a)$$

and $\exp(ia\cos g) = \sum_{q=-\infty}^{\infty} i^q J_q(a)\exp(iqg)$.

Then $S_1 = \exp\left[2p\,iR\left(r_0 - r_g + md\right)\right](S_0 + S_c + S_s)$

where $S_0 = J_0\left(2p\,r_g\frac{h_1}{l}\right)\sum_{q'=-\infty}^{\infty} i^{q'}J_{q'}(2p\,r_g R)\cdot$

$$\cdot\exp(-iq'e)\sum_{t=0}^{T-1}\exp(iq'\Delta e\,t) =$$

$$= J_0\left(2p\,r_g\frac{h_1}{l}\right)\sum_{q'=-\infty}^{\infty} i^{q'}J_{q'}(2p\,r_g R)\exp(-iq'e)G_0(q'\Delta e) \qquad (13)$$

$$S_c = \sum_{q=1}^{\infty}J_{2q}\left(2p\,r_g\frac{h_1}{l}\right)\sum_{q'=-\infty}^{\infty} i^{q'}J_{q'}(2p\,r_g R)\cdot$$

$$\cdot\left\{\exp\left[-i(q'+2q)e\right]G_c\left[(q'+2q)\Delta e\right] + \right.$$

$$\left. + \exp\left[-i(q'-2q)e\right]G_c\left[(q'-2q)\Delta e\right]\right\}, \qquad (14)$$

$$S_s = \sum_{q=0}^{\infty}J_{2q+1}\left(2p\,r_g\frac{h_1}{l}\right)\sum_{q'=-\infty}^{\infty} i^{q'}J_{q'}(2p\,r_g R)\cdot$$

$$\cdot\left\{\exp\left[-i(q'+2q+1)e\right]G_s\left[(q'+2q+1)\Delta e\right] - \right.$$

$$\left. - \exp\left[-i(q'-2q-1)e\right]G_s\left[(q'-2q-1)\Delta e\right]\right\} \qquad (15)$$

Here, as well as earlier, the following sum is used:

$$G(x) = \sum_{m=0}^{M-1}\exp(ixm) = \frac{\sin\frac{Mx}{2}}{\sin\frac{x}{2}}\exp\left[i(M-1)\frac{x}{2}\right] \qquad (16)$$

which has a sharp maximum at *x*, equal to an integer of 2π, the height of a maximum is equal to *M*, and its width is inversely proportional to this value. For example, in the case of S_0: $x = q'\Delta\varepsilon$, $M = T$, the maximum of function is realized at:

$$q' = h_2\frac{2p}{\Delta e} \qquad h_2 = 0;\pm1;\pm2;\pm3;... \qquad (17)$$

However addendum S_1 of the amplitude also contains the multiplier, depending on the index of summation over nanotube layers (over *m*). This summation, after rejection of factors insignificant for this analysis, gives the amplitude multiplier $G(2\pi Rd)$, which looks like (16). Hence, the amplitude of strong reflexes represents a number of addendums, each of which contains the product of the functions of the kind (16): $G(2\pi Rd)$ on the one hand, and one of the functions $G_0(q'\Delta\varepsilon)$, $G_c[(q' \pm 2q)\Delta\varepsilon]$ and $G_s[(q' \pm 2q \pm 1)\Delta\varepsilon]$ – on the other one. Three last functions do not depend on spatial variable *R*, but influence a choice of the members of series over *q*', the Bessel functions of which contain this variable.

Thus, the character of an arrangement of amplitude maxima in a scale *R* depends on the correlation between the widths of the functions of the kind (16), which are determined by parameters *T* and *M*, in each product: the narrower function determines the form and position of diffraction pattern maxima and the wider one modulates their intensities. Let us consider extreme cases of thick and thin radial CSR.

3.1. The Thick Radial CSR (*M* >> *T*)

In this case maxima of the function $G(2\pi Rd)$ are narrow, intensive and positioned in points of its extremum:

$$2p\,Rd = 2p\,l \qquad \Rightarrow \qquad R_l = \frac{l}{d} \quad l = 0, \pm 1, \pm 2, \ldots \qquad (18)$$

It means that the arrangement of strong reflexes is identical on all layer lines of such nanotube. Such microdiffraction pattern is given in Fig. 1 with the only difference, that it belongs not to a circular nanotube, which lattice is considered for analysis simplification, but to the longitudinal monoclinic [2, 3] one. Let us compare the relative intensities of layer lines, determined by addendums S_0, S_c and S_s.

Let us consider addendum S_0. Maxima of the function $G_0(q'\Delta\varepsilon)$ are in the points (17). On the other hand, the main maximum of Bessel function $J_{q'}(2\pi r_g R)$ is close to the value of argument equal to its index, that means, that in the points (18) the main maxima of Bessel functions with $q' = 2\pi r_g l/d$ are positioned. It is obvious that generally this condition cannot be satisfied simultaneously with the condition (17). It means that addendum S_0 practically does not influence the relative intensity of layer lines.

Addendum S_c in the points (18) looks like: $S_c^l = S_{cl}^+ + S_{cl}^-$

where
$$S_{cl}^+ = \sum_{q=1}^{\infty} J_{2q}\left(2p\,r_g\frac{h_1}{l}\right)\sum_{q'=-\infty}^{\infty} i^{q'} J_{q'}\cdot$$
$$\cdot\left(2p\,r_g\frac{l}{d}\right)\exp\left[-i\left(q'+2q\right)e\right]G_c\left[\left(q'+2q\right)\Delta e\right]$$
$$S_{cl}^- = \sum_{q=1}^{\infty} J_{2q}\left(2p\,r_g\frac{h_1}{l}\right)\sum_{q'=-\infty}^{\infty} i^{q'} J_{q'}\left(2p\,r_g\frac{l}{d}\right)\cdot$$
$$\cdot\exp\left[-i\left(q'-2q\right)e\right]G_c\left[\left(q'-2q\right)\Delta e\right]$$

The main maxima of addendum S_{cl}^+ Bessel functions are located close to the points $q' \approx 2\pi r_g l/d$ and $2q \approx 2\pi r_g h_1/\lambda$. On the other hand indexes q' and q are connected with each other by the area of noticeable values of the function $G_c[(q' + 2q)\Delta\varepsilon]$. Its rather wide maximum is in the point $(q' + 2q)\Delta\varepsilon = 2\pi h_2$. Thus, we obtain approximate equality:

$$2p\,r_g\frac{l}{d} + 2p\,r_g\frac{h_1}{l} \approx 2p\,\frac{h_2}{\Delta e} \Rightarrow \qquad h_1 \approx l\left(\frac{h_2}{a} - \frac{l}{d}\right) \qquad (19)$$

As $\lambda \approx Ta$, then in the last equality $h_1 \approx Ta\left(\frac{h_2}{a} - \frac{l}{d}\right) \approx Th_2 - \frac{Ta}{d}l$ the integer value of h_1 is provided only at $l = 0$. In view of (7) it means that the layer line (the basic layer line) is of the greatest intensity and located close to

$$z^* \approx \frac{h_2}{a} \approx \frac{Th_2}{l} \qquad (20)$$

at $h_2 > 0$, as it is observed in Fig. 1.

As maxima of function $G_c[(q' + 2q)\Delta\varepsilon]$ have some width, the layer lines getting in the appropriate interval have also appreciable intensity (additional layer lines). Let us take differential from both parts of (19) at the constant index h_2 that is close to (20):

$$\Delta h_1 \sim -\Delta l \qquad (21)$$

where the approximate equality is replaced with a mark of proportionality, as the interval of intensive layer lines depends on experimental conditions too. From (21) it is visible that the quantity of additional layer lines is proportional to the value of index l also observed in Fig. 1. Addendum S_{cl}^- gives the similar result for $h_2 < 0$.

Addendum S_s in the points (18) looks like $S_s^l = S_{sl}^+ - S_{sl}^-$

where
$$S_{sl}^+ = \sum_{q=1}^{\infty} J_{2q+1}\left(2p\,r_g\frac{h_1}{l}\right)\sum_{q'=-\infty}^{\infty} i^{q'} J_{q'}\cdot$$
$$\cdot\left(2p\,r_g\frac{l}{d}\right)\exp\left[-i\left(q'+2q+1\right)e\right]G_s\left[\left(q'+2q+1\right)\Delta e\right]$$
$$S_{sl}^- = \sum_{q=1}^{\infty} J_{2q+1}\left(2p\,r_g\frac{h_1}{l}\right)\sum_{q'=-\infty}^{\infty} i^{q'} J_{q'}\left(2p\,r_g\frac{l}{d}\right)\cdot$$
$$\cdot\exp\left[-i\left(q'-2q-1\right)e\right]G_s\left[\left(q'-2q-1\right)\Delta e\right]$$

Maxima of Bessel functions in S_{sl}^+ take place under conditions: $q' \approx 2\pi r_g l/d$ and $2q + 1 \approx 2\pi r_g h_1/\lambda$, and maximum of function $G_s[(q' + 2q)\Delta\varepsilon]$ is in the point $(q' + 2q + 1)\Delta\varepsilon = 2\pi h_2$, that gives again (19) and all its consequences.

3.2. The Thin Radial CSR ($M < T$)

The basis for such model consideration is the diffraction pattern in Fig. 2, radially lengthened basal reflexes of which allow to speak about the small CSR sizes in this direction. In this case maxima of functions $G_0(q'\Delta\varepsilon)$, $G_c[(q' \pm 2q)\Delta\varepsilon]$ and $G_s[(q' \pm 2q \pm 1)\Delta\varepsilon]$ in (13), (14) and (15), correspondingly, are narrower and intensive, than those of $G(2\pi Rd)$, and it is possible to be limited to their peak values.

Let us consider an addendum S_0 at peak value of q' from (17).

$$S_0(h_2) \approx i^{q'} T J_0\left(2p\,r_g\frac{h_1}{l}\right)J_{q'}\left(2p\,r_g R\right)\exp\left(-iq'e\right)$$

Main maximum of the second Bessel function takes place at:

$$2p\,r_g R \approx q' = h_2\frac{2p}{\Delta e} \qquad \Rightarrow \qquad R_{h_2} \approx \frac{h_2}{a}$$

But on the other hand the summation over layers (over m) gives condition (18) again, though with a little wider maxima. However it is obvious that in this case

these two conditions are incompatible too. Hence, addendum S_0 has not essential influence on positions of strong reflexes.

A condition of the maximum of functions $G_c[(q' \pm \pm 2q)\Delta\varepsilon]$ included in S_c looks like:

$$(q' \pm 2q)\Delta e = 2p\,h_2 \qquad \Rightarrow \qquad 2q = \pm\left(\frac{2p\,h_2}{\Delta e} - q'\right)$$

and function S_c, under this condition, $S_{ch_2} = S^+_{ch_2} + S^-_{ch_2}$

where $S^+_{ch_2} = T(-1)^{Th_2} \sum_{q'=-\infty}^{\infty} i^{q'} J_{q'}(2p\,r_g R) J_{\frac{2p\,h_2}{\Delta e} - q'}\left(2p\,r_g \frac{h_1}{l}\right)$

$$S^-_{ch_2} = T(-1)^{Th_2} \sum_{q'=-\infty}^{\infty} i^{q'} J_{q'}(2p\,r_g R) J_{-\frac{2p\,h_2}{\Delta e} + q'}\left(2p\,r_g \frac{h_1}{l}\right)$$

and is used: $\varepsilon/\Delta\varepsilon \approx T/2$. As before, let us write down for $S^+_{ch_2}$ the approximate equality from conditions of Bessel functions maxima at the peak value (18) of functions $G(2\pi Rd)$:

$$2p\,r_g \frac{h_1}{l} \approx 2p\,\frac{h_2}{\Delta e} - 2p\,r_g \frac{l}{d} \Rightarrow h_1 \approx l\left(\frac{h_2}{a} - \frac{l}{d}\right)$$

We have again obtained (19), that means, as in this case the basic layer line is close to z^*, determined by (20), too. However the function $G(2\pi Rd)$ in this case is a modulating one, the positions of peaks on the layer line are determined by maxima of function $G_c[(q' + 2q)\Delta\varepsilon]$. Then, substituting the current value of argument R instead of its peak value l/d in the latter equality, we obtain:

$$R^{h_1}_{h_2} \approx \frac{h_2}{a} - \frac{h_1}{l}$$

This expression differs from its analogue (18) for the case of thick radial CSR in two aspects. First, the positions of strong reflexes on the layer line are determined not by "basal" interlayer spacing d, but "longitudinal" lattice parameter a. Secondly, the positions of all series displaces on the distance h_1/λ at transition from one layer line to another, that is observed on the diffraction pattern in Fig. 2.

Expression (21) that is also observed on the diffraction pattern in Fig. 2 gives again the estimation of interval width near the value (20), in which the additional layer lines take place, similar to the previous item.

Addendum S_2 from (11) gives similar expressions for other combination of indexes h_1, h_2 and l signs.

4. Conclusions

The analysis of strong reflexes formed from the offered multiwall circular orthogonal mixed-layer goffered nanotube lattice model, consisting of alternating layers of type *A* and *B*, has shown:

1. All reflexes are located on the system of layer lines $z^* = h_1/\lambda$, where h_1 – index of layer line (integer), and λ – period of goffering. However the greatest intensity has reflexes of basic layer lines, which are close to value z^* appropriate to the coordinated longitudinal period ***a, i.e.*** $z^* = h_2/a$, where h_2 – integer.

2. With the increase of the strong reflex index l the intensity of additional layer lines become appreciable, so the width of the layer lines interval (lengthways z^*) having appreciable intensity is proportional to this index.

3. In the case of thick radial CSR the strong reflexes are located on the layer line as those from not goffered lattice. In the case of thin radial CSR the series of strong reflexes are displaced lengthways a layer line depending on its index h_1.

Acknowledgements

Authors thank Dr. R. Tenne for nanotube images and microdiffraction patterns.

References

[1] Radovsky G., Popovitz-Biro R., Staiger M. *et al.*: Angew. Chem. Intl. Ed., 2011, **50**, 12316.
[2] Nasyrov I., Pashin D., Khalitov Z. and Valeeva D.: Sci. Israel Techn. Adv., 2010, **12**, 63.
[3] Figovsky O., Pashin D., Nasyrov I. *et al.*: Chem. & Chem. Techn., 2011, **6**, 43.

ЦИЛІНДРИЧНІ НАДРЕШІТКИ SnS/SnS_2: МОДЕЛЬ СТРУКТУРИ ТА ДИФРАКЦІЯ

Анотація. *Створено циліндричні надрешітки на основі змішано-шарових нанотрубок SnS/SnS_2. Надперіод утворюється внаслідок повздовжнього гофрування структури нанотрубки завдяки несіврозмірності решіток циліндричних шарів SnS і SnS_2. Запропонована проста модель структури, проаналізовані специфічні дифракційні ефекти.*

Ключові слова: *нанотрубка, гофрована нанотрубка, надрешітка.*